The roles of FGF signaling in germ cell migration in the mouse

Yutaka Takeuchi[1], Kathleen Molyneaux[2], Chris Runyan[3], Kyle Schaible[3] and Chris Wylie[3,*]

[1]Department of Marine Biosciences, Tokyo University of Marine Science and Technology, 4-5-7 Konan, Minato-ku, Tokyo 108-8477, Japan
[2]Department of Genetics, School of Medicine, Case Western Reserve University, Cleveland, OH 44106, USA
[3]Division of Developmental Biology, Cincinnati Children's Hospital Research Foundation, Cincinnati, OH 45229, USA
*Author for correspondence (e-mail: Christopher.Wylie@cchmc.org)

Accepted 8 September 2005

Development 132, 5399-5409
Published by The Company of Biologists 2005
doi:10.1242/dev.02080

Summary

Fibroblast growth factor (FGF) signaling is thought to play a role in germ cell behavior. FGF2 has been reported to be a mitogen for primordial germ cells in vitro, whilst combinations of FGF2, steel factor and LIF cause cultured germ cells to transform into permanent lines of pluripotent cells resembling ES cells. However, the actual function of FGF signaling on the migrating germ cells in vivo is unknown. We show, by RT-PCR analysis of cDNA from purified E10.5 germ cells, that germ cells express two FGF receptors: *Fgfr1-IIIc* and *Fgfr2-IIIb*. Second, we show that FGF-mediated activation of the MAP kinase pathway occurs in germ cells during their migration, and thus they are potentially direct targets of FGF signaling. Third, we use cultured embryo slices in simple gain-of-function experiments, using FGF ligands, to show that FGF2, a ligand for FGFR1-IIIc, affects motility, whereas FGF7, a ligand for FGFR2-IIIb, affects germ cell numbers. Loss of function, using a specific inhibitor of FGF signaling, causes increased apoptosis and inhibition of cell shape change in the migrating germ cells. Lastly, we confirm in vivo the effects seen in slice cultures in vitro, by examining germ cell positions and numbers in embryos carrying a loss-of-function allele of FGFR2-IIIb. In FGFR2-IIIb$^{-/-}$ embryos, germ cell migration is unaffected, but the numbers of germ cells are significantly reduced. These data show that a major role of FGF signaling through FGFR2-IIIb is to control germ cell numbers. The data do not discriminate between direct and indirect effects of FGF signaling on germ cells, and both may be involved.

Key words: Germ cells, FGF signaling, ERK

Introduction

The germ line arises in the mouse embryo as a small group of primordial germ cells (PGCs), which pass through the posterior primitive streak during gastrulation and occupy the hind gut as it forms from the posterior definitive endoderm. At E9.5, the PGCs emigrate from the hind gut, migrate laterally through the dorsal body wall mesenchyme in left and right streams, and then aggregate into clusters in the genital ridges, where they co-assemble with somatic cells of the genital ridges to form the sex cords of the gonads (Molyneaux and Wylie, 2004). During their migration, abundant evidence shows that germ cell behavior in the mouse is controlled by signaling molecules released by the surrounding cells (Godin et al., 1990). Germ cell survival, both in vitro and in vivo, requires interaction between steel factor in the environment, and its receptor Kit (also known as c-Kit), expressed by the germ cells (Bennett, 1956; Mintz and Russell, 1957; Godin et al., 1991). Directional migration requires interaction between SDF1 in the environment and its receptor CXCR4 expressed by germ cells (Molyneaux et al., 2003). Many purified growth factors, agonists and antagonists have been shown to affect the motility, survival and proliferation of cultured germ cells (De Felici, 2000). However, genetic evidence exists for only some of these.

The FGF family of signaling ligands is known to control many aspects of development, including growth, differentiation and migration (Powers et al., 2000). FGF signaling is complex, and involves four receptors (FGFR1-FGFR4). In FGFR1-FGFR3, alternative splicing of the carboxy-terminal half of the Ig domain III yields 'IIIb' and 'IIIc' forms of the receptor, which have distinct expression patterns and ligand specificities. 'IIIb' forms are thought to be epithelially expressed and activated by mesenchymally produced FGFs, whereas 'IIIc' forms are usually mesenchymal and activated by epithelial FGFs. Therefore, a total of seven receptors bind with varying affinities and specificities to at least 22 distinct FGF ligands, four of which are thought to be non-signaling (Ornitz and Itoh, 2001).

FGF signaling is thought to be important in germ cell behavior during migration. FGF2 has been reported to act as a mitogen for PGCs in vitro, and, together with steel factor and LIF, causes cultured germ cells to change into pluripotential permanent cell lines (Matsui et al., 1992). Furthermore, radiolabeled FGF2 binds to PGCs in culture, suggesting the presence of FGF receptors (FGFRs) (Resnick et al., 1998). However, the FGFR combinations expressed by germ cells, the ligands they respond to, and their individual or collective roles in germ cell behavior are not known.

We show, using RT-PCR from flow-cytometry-purified germ cells, that germ cells express the FGF receptors FGFR1-IIIc

and FGFR2-IIIb during migration. Antibodies specific to the di-phosphorylated forms of ERK1 and ERK2 (dp-ERK1/2) have been shown to be reliable markers of activity of the MAP kinase pathway in the mouse embryo (Corson et al., 2003). In addition, by using inhibitors of FGF signaling, and of MEK1/2, which phosphorylates ERK1/2 in the MAP kinase pathway, we show that di-phosphorylation of ERK1/2 in migrating germ cells is mediated, either directly or indirectly, by FGF signaling.

Gain- and loss-of function experiments using embryo slices, together with time-lapse analysis of PGC migration, show that FGF signaling is required to maintain both motility and normal germ cell numbers during migration, but not for their migration to the genital ridges nor their proliferation during migration. This result was confirmed in vivo by examining the effects of a targeted mutation of FGFR2-IIIb, which causes reduced numbers of germ cells to colonize the genital ridges, and increased apoptosis of germ cells.

Materials and methods

Mouse breeding, embryo preparation and genotyping

Mouse embryos were generated by crossing OCT4ΔPE:GFP transgenic males (Anderson et al., 1999) with CD1 females. In this transgenic embryo, migrating and gonadal PGCs express EGFP under the control of OCT4ΔPE regulatory sequences. Mice with a floxed allele of FGFR2-IIIb have been described elsewhere (De Moerlooze et al., 2000). pCAGGS-Cre mice (Araki et al., 1995), which express Cre ubiquitously, were used to generate global heterozygous embryos (FGFR2-IIIb$^{flox/\Delta}$). Then, FGFR2-IIIb$^{flox/\Delta}$ animals were crossed to the OCT4ΔPE:GFP line of mice to generate FGFR2-IIIb$^{wt/\Delta}$; OCT4ΔPE:GFP$^{+/-}$ mice. Global FGFR2-IIIb-targeted embryos carrying the OCT4ΔPE:GFP gene were recovered from matings between FGFR2-IIIb$^{flox/\Delta}$ and FGFR2-IIIb$^{wt/\Delta}$; OCT4ΔPE:GFP$^{+/-}$. Genomic DNA was isolated from tails (adults) and heads (embryos), and their genotypes determined by PCR. Primers used for FGFR2-IIIb (forward, 5′-CTGCCTGGCTCACTGTCC-3′; reverse, 5′-CTCAACAGGCATGCAAGGTC-3′) generate a 350-base-pair (bp) fragment from the FGFR2-IIIb wild-type allele and a 400-bp fragment from the FGFR2-IIIb floxed allele. Absence of fragments was diagnostic of the FGFR2-IIIb Δ allele. Primers specific for the GFP gene (forward, 5′-GCGAAGCTTACCATGGGTAAAGGAGAAGA-3′; reverse, 5′-GCAGGTACCTTATCTGAGTCCGGACTTGTATA-3′) were used as an internal positive control. The PCR protocol was 5 minutes at 94°C, then 35 cycles of 30 seconds at 94°C, 30 seconds at 58°C and 30 seconds at 72°C, followed by a 10-minute extension step at 72°C. All animals were treated according to protocols approved by the Institutional Animal Care and Use Committee at Cincinnati Children's Hospital.

Chip analysis, RT-PCR and DNA sequencing

Gene expression profiles of E10.5 PGCs using the Affymetrix MG-U74Av2 were reported previously (Molyneaux et al., 2004). Chip analysis was performed using MicroArray Suite software (Affymetrix) to statistically determine 'presence' and 'absense' calls. For RT-PCR analysis, total RNA was isolated from FACS-purified E10.5 PGCs using RNeasy Protect Mini Kit (Qiagen). Twenty-five ng of total RNA was reverse transcribed using SuperScript First-Strand Synthesis System (Invitrogen). PCR was performed in a 15-μl volume using Redmix Plus (2.0 mM $MgCl_2$) (GeneChoice) as a source of Taq, buffer and dNTPs. PCR reactions were performed as described above. Products from PCR amplifications were cloned into the pGEM-T easy vector (Takara) and subjected to DNA sequencing.

Primers used were as follows:

stella (*Dppa3* – Mouse Genome Informatics), 5′-TGAGTTTGAACGGGACAGTG-3′ (forward) and 5′-GATTTCCCAGCACCAGAAAA-3′ (reverse);

steel (*Kitl* – Mouse Genome Informatics), 5′-AATGCACAACTGCCATCTCC-3′ (forward) and 5′-AGGAATGCCTAGACTACTGGAAAA-3′ (reverse);

Twist1, 5′-CCCCACTTTTTGACGAAGAA-3′ (forward) and 5′-GATTTGCAGGCCAGTTTGAT-3′ (reverse);

Odc, 5′-GCCATTGGGACAGGATTTGAC-3′ (forward) and 5′-CATCATCTGGACTCCGTTACTGG-3′ (reverse);

Fgfr1, 5′-CTTGACGTCGTGGAACGATCT-3′ (common forward), 5′-CACGCAGACTGGTTAGCTTCAC-3′ (*IIIb* reverse) and 5′-AGAACGGTCAACCATGCAGAG-3′ (*IIIc* reverse);

Fgfr2, 5′-CCCATCCTCCAAGCTGGACTGCCT-3′ (common forward), 5′-CAGAGCCAGCACTTCTGCATTG-3′ (*IIIb* reverse) and 5′-CAGAACTGTCAACAATGCAGAGTG3′ (*IIIc* reverse);

Fgfr3, 5′-CAAGTTTGGCAGCATCCGGCAGAC-3′ (common forward), 5′-TCTCAGCCACGCCTATGAAATTGGTG-3′ (*IIIb* reverse) and 5′-CACCACCAGCCACGCAGAGTGATG-3′ (*IIIc* reverse); and

Fgfr4, 5′-TTCTGTTCCAGCCTTATGCCCC-3′ (forward) and 5′-TGATGCCCCTTTCACCAAGATG-3′ (reverse).

Embryo slice culture

Transverse slices from the hind gut regions of mouse embryos were cultured and filmed as previously described (Molyneaux et al., 2003). Briefly, E9.5 embryos were manually sliced to 1.5- to 2-somites width by using surgical blades. Slices were put on the Collagen IV-treated culture inserts (Millipore) and incubated in DMEM/F-12 medium (Gibco BRL) with 0.04% lipid-free BSA (Sigma) and 100 U/ml penicillin-streptomycin solution (Sigma). To analyze the effect of FGF signaling, purified recombinant FGF2 (R&D Systems) and FGF7 (Peprotech), and soluble inhibitors for FGF signaling [MEK inhibitor U0126 (Cell signaling), FGFR inhibitor SU5402 (Calbiochem)] were added at the indicated concentrations. Because these inhibitors were dissolved in DMSO, the same amount of DMSO was added to control groups.

Time-lapse analysis of migrating germ cells

Slices were filmed using the Zeiss LSM 510 confocal system. Images were captured every 7 minutes for 700 minutes. Movies were analyzed using NIH image, as previously described (Molyneaux et al., 2001). For counting PGCs in slices, the tissue was optically sectioned in 15 μm steps (with a 5 μm overlap). PGCs were counted in individual optical sections by using the overlay feature in the Zeiss software to mark cell positions. Three to six independent repeat experiments were performed to obtain means and standard errors of the mean (s.e.m.), and Tukey's HSD test was used to identify significant differences between controls and each treatment.

BrdU incorporation assay

Incorporation of bromodeoxyuridine (BrdU) into PGCs was assayed using the Amersham Cell Proliferation Kit (RPN20). E9.5 embryo slices containing migrating PGCs were treated with FGF2, FGF7 or FGFR inhibitor for 6 hours. Slices were treated with 0.1% BrdU labeling reagent for an additional 2 hours in the presence of FGF ligands and inhibitor. At the end of the culture period, the slices were rinsed with PBS, fixed in 4% paraformaldehyde (PFA) overnight at 4°C, rinsed with PBS containing 0.1% Triton X-100 (PBST), then processed for frozen sectioning. In a single experiment, eight slices dissected from three to four embryos were used for each treatment. Each experiment was repeated three times to obtain means and the s.e.m. of the percentages of BrdU-positive PGCs, and Tukey's HSD test was used to identify significant differences between controls and each treatment. For the in utero labeling of embryos, pregnant females at 11.5 days post coitus received an i.p. injection of 500 μl of 100% BrdU labeling reagent and were pulsed for 4 hours. The harvested

embryos were fixed in 4% PFA (overnight, 4°C), then processed for frozen sectioning.

Immunofluorescence analysis on whole-mount embryo slices or frozen sections

Whole-mount dp-ERK1/2 staining was performed on PGC-containing embryo slices dissected from E9.5 embryos. Slices were fixed in 4% PFA overnight at 4°C, and rinsed with PBST. Slices were blocked overnight in blocking buffer (2% horse serum/2% IgG-free BSA in PBS), treated with a 1:100 diluted anti-dp-ERK1/2 monoclonal antibody (Sigma) overnight, washed for 1 hour (4×) in PBST, and treated with 15 μg/ml Cy5-conjugated anti-mouse IgG antibody (Jackson ImmunoResearch Laboratories) in the blocking buffer overnight in the dark. Tissues were washed as described and mounted in 75% glycerol with 100 μg/ml DABCO (Sigma). All procedures were performed at 4°C.

The immunostaining of embryo slices or embryonic gonads with anti-OCT3/4 donkey IgG (1:100; R&D Systems), anti-BrdU mouse monoclonal (1:100; Amersham) and anti-cleaved caspase 3 rabbit IgG (1:1000; Cell Signaling) antibodies was performed on frozen sections. Samples were embedded in OCT medium (Triangle Biomedical Sciences) and 14-μm sections cut. Sections were washed in PBST for 20 minutes, blocked for 1 hour in the blocking buffer, and then incubated with diluted primary antibodies in the blocking buffer overnight. Slides were washed for 5 minutes (3×) with PBST and incubated with the appropriate 15 μg/ml Cy5-conjugated secondary antibodies (Jackson ImmunoResearch Laboratories). Slides were washed as described above and mounted in glycerol with DABCO. All procedures were performed at room temperature. Images were captured using a Zeiss LSM 510 confocal system.

In order to obtain the density of germ cell numbers in the genital ridges, the area of the genital ridge was measured using the LSM software and multiplied by the thickness of image, to give the volume of genital ridges in *z*-stack confocal image series. Then, the number of germ cells was divided by the volume of genital ridge. A total of three independent litters were assayed to obtain the means and s.e.m. of the density of gonadal germ cells. Tukey's HSD test was used to identify significant differences between wild-type and *Fgfr2-IIIb* null embryos.

Alkaline phosphatase staining of germ cells

E11.5 embryos were fixed overnight in 4% PFA at 4°C, and washed thoroughly in PBS. The genital ridges were excised and incubated for 2 hours in permeabilization buffer (0.1% SDS, 1% Triton X-100 in PBS), then rinsed for 10 minutes (3×) in Tris-maleate (pH 9.0) buffer. The permeabilized genital ridges were incubated in alkaline phosphatase buffer [0.4 mg/ml Naphthol AS-MX phosphate (Sigma, N-5000), 1 mg/ml Fast Red TR salt (Sigma, F2768) in Tris-maleate buffer] for 20 minutes. Samples were placed in 50% glycerol/PBS and photographed using a dissecting microscope equipped with a digital camera.

Results

Germ cells express two FGF receptors during migration

To determine which FGFRs are expressed by migrating mouse PGCs purified from E10.5 embryos, we first analyzed their expression patterns using the Affymetrix array analysis of germ cell gene expression reported previously (Molyneaux et al., 2004). On the two independent chips, we found that *Fgfr2* was scored as present in both chips (data not shown).

The oligonucleotides used on this chip do not distinguish between the two splice variants *Fgfr2-IIIb* and *Fgfr2-IIIc*. To analyze further the expression of FGF receptors, we dissected genital ridges, the dorsal body wall, and the hind gut mesentery, as a single piece, from OCT4ΔPE:GFP embryos, in which the migrating germ cells express high levels of GFP (Anderson et al., 1999). Tissues were dissociated, and separated by flow cytometry into germ cell (GFP-positive) and somatic cell (GFP-negative) populations. cDNA was made from the two cell populations. The purity of the preparations was analyzed by the presence of the germ cell marker stella, and the somatic cell markers steel and *Twist1*. As shown in Fig. 1A, stella was found to be present in PGC cDNA, but steel and *Twist1* were absent. This observation confirmed that signals from these RT-PCR experiments are reliable in identifying genes expressed by migrating PGCs. Preparations were chosen for further analysis in which the germ cell cDNA contained no detectable steel or *Twist1*, and the somatic cells contained no detectable stella. PCR primers were designed to identify all of the FGF receptors, including their splice variants. As shown in Fig. 1B, germ cells were found to express *Fgfr2-IIIb* during migration. In addition, we found that *Fgfr1-IIIc* was also expressed by migrating germ cells. Products obtained from the RT-PCR amplifications were of the predicted sizes (i.e. *Ffgr1-IIIb*, 323 bp; *Fgfr1-IIIc*, 343bp; *Fgfr2-IIIb*, 215 bp; *Fgfr2-IIIc*, 314 bp). PGC-derived PCR products were sequenced to verified that these bands truly represented the expression of both *Fgfr2-IIIb* and *Fgfr1-IIIc* in the PGCs (data not shown).

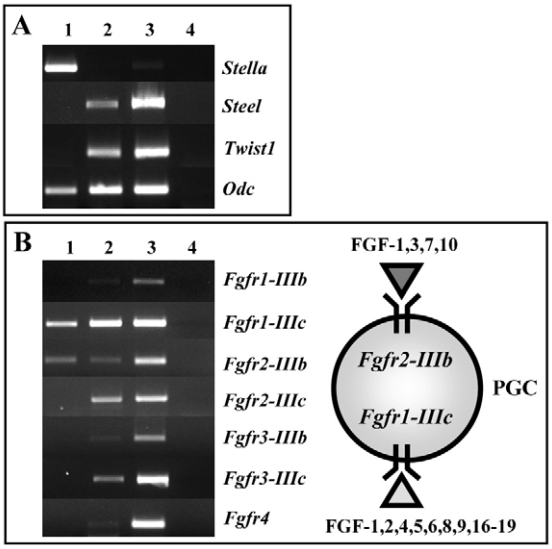

Fig. 1. *Fgfr1-IIIc* and *Fgfr2-IIIb* isoforms are expressed by migrating PGCs. (A) cDNA prepared from FACS-sorted E10.5 PGCs and somatic cells was subjected to PT-PCR. The purity of the preparations was confirmed by expression of the PGC marker gene stella, and the somatic marker genes steel and *Twist1*. Lane 1, E10.5 PGC cDNA (PGC); Lane 2, E10.5 somatic cell cDNA (SC); Lane 3, E10.5 whole embryo cDNA (WE); Lane 4, RT(–) E10.5 whole embryo cDNA [WE(RT-)]. (B) The expression patterns of all FGFR isoforms were assayed by RT-PCR. *Fgfr1-IIIc* and *Fgfr2-IIIb* were found to be expressed by E10.5 PGCs (lane 1; lanes as in A). PGC-derived PCR products were sequenced and verified that these bands truly represented the expression of each FGFR. The illustration shows the potential FGF ligands that could activate each FGFR.

FGF-mediated ERK1/2 activation occurs in migrating germ cells

An antibody specific for activated (di-phosphorylated) ERK1/2 (anti-dpERK1/2) was used to stain fixed trunk regions

(between the fore and hind limb buds) of E9.5 OCT4ΔPE:GFP embryos. In order to verify that staining was specific for dpERK1/2, samples were incubated for 4 hours before fixation with or without a chemical inhibitor of MEK (U0126), which blocks the MAPK kinases (MEK1/2) responsible for phosphorylation of ERK1/2. Fixed tissues were cut into transverse slices, stained, and examined under the confocal microscope. As shown in Fig. 2A, dp-ERK1/2 staining was significantly reduced in E9.5 embryos treated with the MEK inhibitor.

Analysis of the embryos under higher magnification (Fig. 2B-D) revealed cytoplasmic staining of PGCs in the absence of MEK inhibitor. Cells that were both dp-ERK1/2-positive, and GFP-positive, were scored as dp-ERK1/2-positive germ cells. In three independent preparations from E9.5, 49% of germ cells were positive for dp-ERK1/2 (Fig. 2C,I). The same proportion of PGCs was dp-ERK1/2 positive at E10.5 (data not shown). This suggests the ERK1/2 activation may be transient, either because it is cell cycle dependent, or because of a transient presence of signal. The pattern of dp-ERK1/2 staining and the percentage of dp-ERK1/2 positive PGCs in freshly isolated and fixed wild-type embryos was comparable with embryos cultured for four hours in DMSO, indicating that the dp-ERK1/2 staining seen in these experiments was not an artifact of the culture system. The staining was diminished by MEK inhibitor treatment. Only 12% of PGCs were dp-ERK1/2 positive in U0126-treated embryos (Fig. 2D,I).

To test whether positive staining indicates activation of the MAP kinase pathway by FGF signaling, rather than through a different receptor pathway, slices were incubated with either

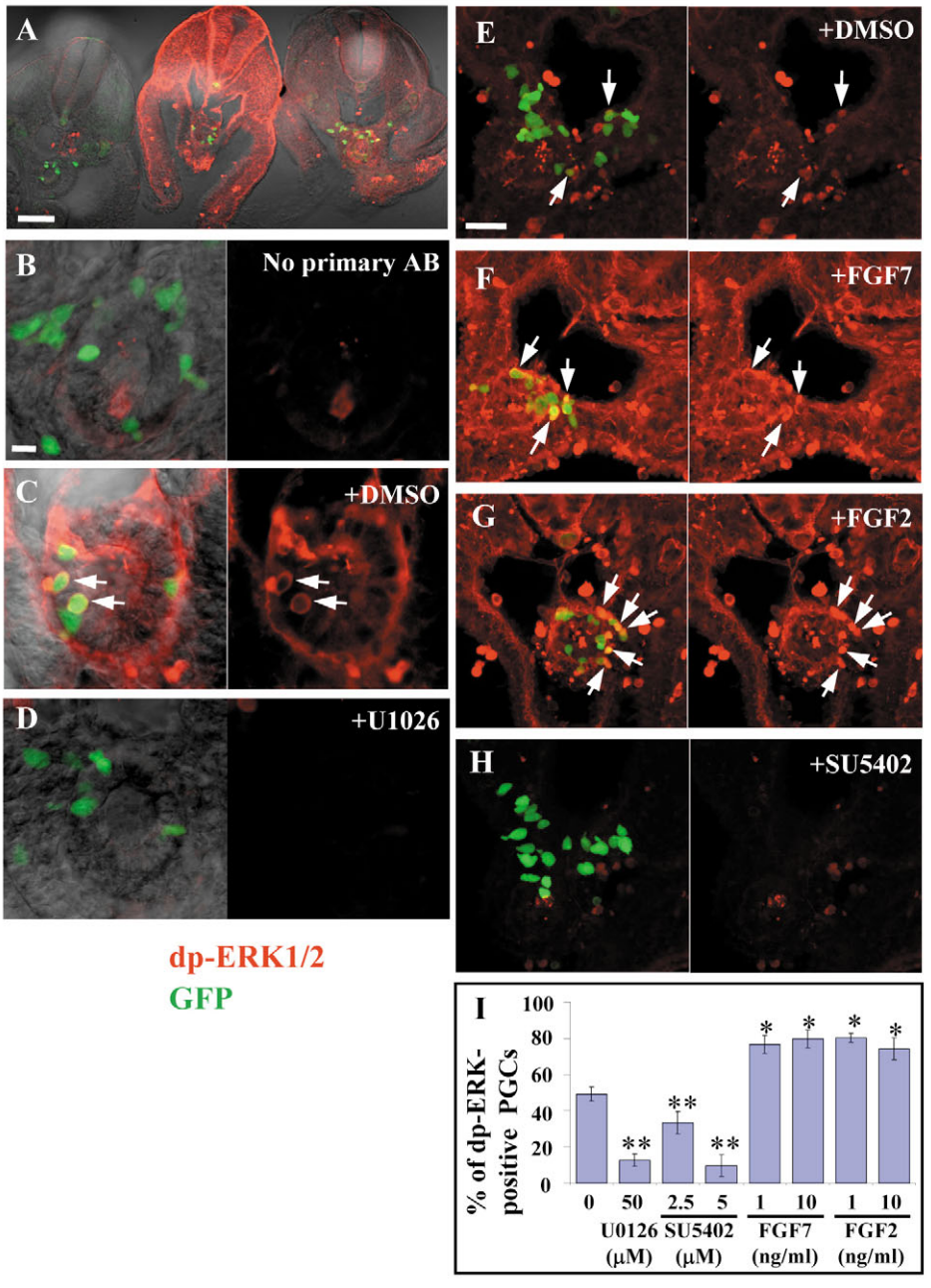

Fig. 2. FGFR-ERK1/2 signaling is activated in migrating PGCs. (A) Whole-mount dp-ERK1/2 (red) staining in transverse slices from E9.5 OCT4ΔPE:GFP embryos; germ cells are shown in green. To show the specificity of the dp-ERK1/2 antibody, trunk regions of embryos were cultured with (right) or without (center) MEK inhibitor (50 μM of U0120) for 4 hours, fixed, sliced and stained for dp-ERK1/2. Slices in which the primary antibody was left out of the protocol (left) were used as negative controls. (B-D) Higher magnification views of hind gut regions of the embryos shown in A. Confocal sections reveal that cytoplasmic staining observed in PGCs of the control slice (arrowheads in C) was diminished in the U0126-treated slice (D) and the negative control slice (B). (E-H) The percentage of dp-ERK1/2-positive PGCs was dramatically affected by 4-hour treatments of FGFs (FGF7 and FGF2) or FGFR inhibitor (SU5402). (E) Dp-ERK1/2 staining of control embryo cultured with DMSO. The numbers of dp-ERK1/2-positive PGCs (red; arrows) were increased in embryos incubated with (F) 10 ng/ml of FGF7 or (G) 10 ng/ml of FGF2, and decreased in embryos treated with (H) 5 μM of SU5402. (B-H) dp-ERK1/2 images are on the right; GFP overlaid image, left. (I) The percentage of dp-ERK1/2-positive PGCs obtained from each treatment is summarized. Error bars show the s.e.m. Asterisks indicate the degree of statistical significance (P<0.01), of increase (*) and decrease (**) compared with the controls. Scale bars: in A, 200 μm; in B, 20 μm for B-D; in E, 40 μm for E-H.

FGF ligands or an inhibitor of FGFR tyrosine kinase activity (SU5402). SU5402 binds the ATP-binding site of FGFR, and has been reported to inhibit both FGFR1 and FGFR2 phosphorylation (Mohammadi et al., 1997; Bernard-Pierrot et al., 2004). Addition of either FGF2 or FGF7, which are the high-affinity ligands for FGFR1-IIIc and FGFR2-IIIb, respectively (Ornitz and Itoh, 2001; Sher et al., 2003), significantly increased (P<0.01) the percentage of dp-ERK1/2-positive germ cells to 74-80%, whereas the FGFR inhibitor significantly reduced (P<0.01) this number to 10-31% (Fig. 2E-I). This shows that FGF-dependent activation of the MEK-ERK signaling is occurring in migrating PGCs.

FGF signaling controls germ cell number during migration

The fact that germ cells continue to migrate out of the hind gut and into the genital ridges in slice cultures from OCT4ΔPE:GFP embryos, allows a rapid functional assay for the roles of signaling pathways by the addition of ligands, agonists and antagonists to the slices (Molyneaux et al., 2001; Molyneaux, 2003). As an initial test of the role of FGF signaling, transverse slices from the hind gut regions of E9.5 OCT4ΔPE:GFP embryos were cultured for 18 hours in serum-free medium, either in the presence of FGF2 (0.1, 1, 10 ng/ml), FGF7 (1, 10, 100 ng/ml), or SU5402 (1, 5, 10 μM). FGF2 and FGF7, the high-affinity ligands for FGFR1-IIIc and FGFR2-IIIb, respectively, are each thought not to activate the other receptor. Effective doses for FGF2 and FGF7 are described as 100-250 ng/ml and <1000 ng/ml, respectively, in the manufacture's protocol, other published FGF studies have used a wide range of concentrations for these ligands, from 1-1000 ng/ml (Resnick et al., 1998; Weksler et al., 1999; Bridges et al., 2003; Kawase et al., 2004). Because FGF ligand-receptor interactions are influenced by many factors other than ligand concentration, such as heparin and cell-surface proteoglycans, it is impossible to determine what ligand concentrations in vitro will mimic physiological conditions. Therefore, we estimated the lowest effective doses of these reagents that would increase dp-ERK1/2 staining in our slice culture system. We used dose ranges starting at these concentrations. FGF2 had no effect on germ cell numbers in the dose range 0.1-10 ng/ml. Doses of 100 ng/ml caused spreading of the slices and loss of morpholgy. FGF7 caused increased germ cell numbers, when compared with controls, at all doses between 1 and 100 ng/ml. However, only the 100 ng/ml dose was significant at the P=0.05 level. The FGF receptor inhibitor SU5402 caused a dose-dependent decrease in germ cell numbers (Fig. 3A). These data suggest that FGF signaling, either directly on germ cells, or indirectly via somatic cells, controls germ cell numbers during migration.

To test the role of FGF signaling on mitosis of migrating PGCs, embryo slices were exposed to BrdU for 2 hours, followed by a 6-hour incubation with FGF ligands or the inhibitors. Cells that were both BrdU positive, and GFP positive, were scored as BrdU-positive germ cells. The percentage of BrdU-positive PGCs was counted in eight embryo slices from each of two separate experiments for every treatment. As shown in Fig. 3B, levels of BrdU incorporation are not significantly affected by either the FGF ligands or the inhibitor.

To test the basis of the loss of germ cell numbers by

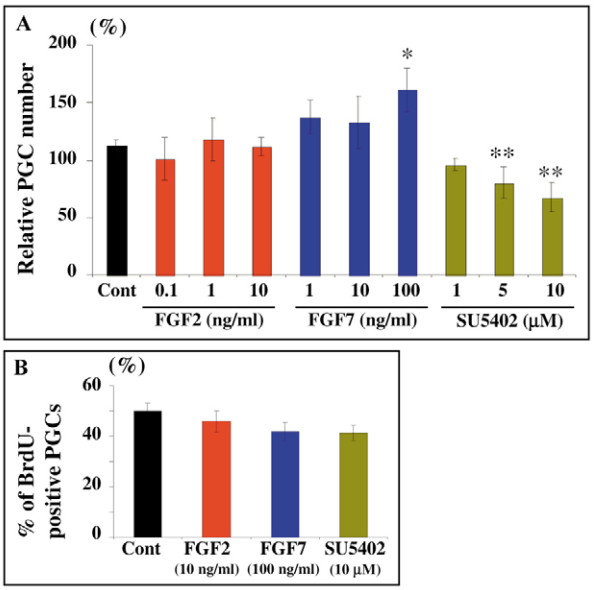

Fig. 3. Effects of adding FGFs or FGFR inhibitor on the numbers of PGCs in E9.5 slice cultures. (A) 'Relative PGC number' represents the number of PGCs at the end of the culture period (18 hours) expressed as a percentage of the number at the start of the culture period in the same slice. Relative PGC number is significantly increased by 100 ng/ml of FGF7 treatment, but significantly reduced by 10 μM of SU5402. FGF2 treatments do not affect PGC numbers. (B) The proliferation of PGCs was quantified by BrdU incorporation assay in cultured slices. Slices, 6-hour pre-cultured with FGF or FGFR inhibitor, were exposed to BrdU for 2 hours. PGCs in the FGF7-, FGF2- and SU5402-treated slices incorporate BrdU at rates comparable with those in the control slices. Each bar shown in A and B shows the mean±s.e.m. obtained from 14-18 slices from triplicate experiments. Asterisks show the degree of statistical significance (P<0.05) of increase (*) and decrease (**) compared with the controls.

SU5402-treatment, we analyzed the degree of germ cell apoptosis in slice cultures. Embryo slices were cultured on the stage of the confocal microscope and time-lapse analysis was performed. Each movie consisted of 100 frames, taken at 7-minute intervals to enable the analysis of germ cell positions in the slices. It is known that, during migration, germ cells in the midline of the embryo die by apoptosis (Pesce et al., 1993). This process is visible in movies of slice cultures from OCT4ΔPE:GFP embryos as a rapid fragmentation and disappearance of GFP-labeled germ cells (Fig. 4A) (see also Stallock et al., 2003). The fact that fragmentation is due to apoptosis was shown by cleaved caspase-3 staining (Fig. 4B), and by the fact that fragmentation does not occur in embryo slices from null mutants of the pro-apoptotic gene BAX (Stallock et al., 2003). We therefore analyzed the timing of fragmentation events in embryo slices treated with SU5402 and recorded the onset of each fragmentation as a single dot (Fig. 4D). For example, the PGC arrowed in Fig. 4A, in a slice treated with 1 μM SU5402, started to fragment at Frame 62. This time of onset of fragmentation is represented as the single dot, circled in red, in Fig. 4D. For each treatment, a total of 10 movies from three independent experiments were analyzed, and all records were summarized in a single figure. Germ cells fragmented throughout the culture period, showing that

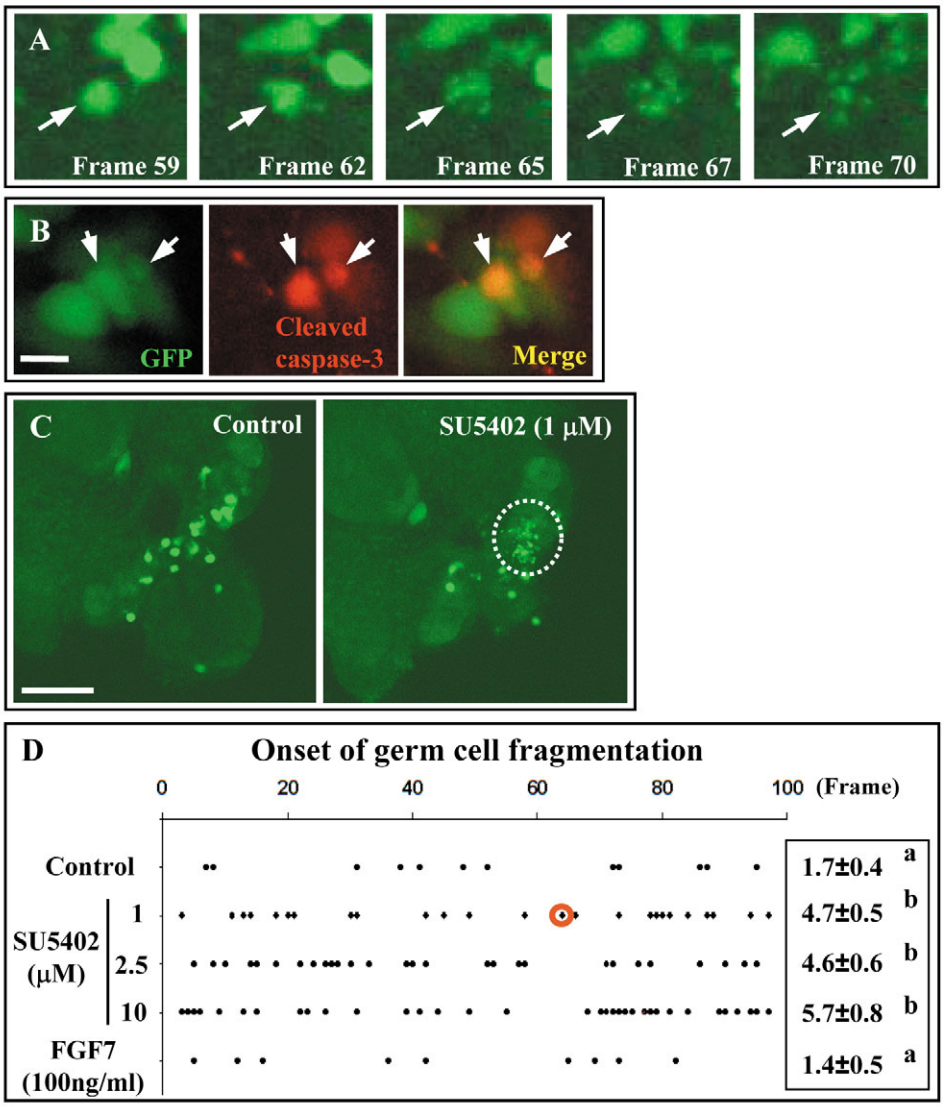

Fig. 4. Fragmentation of migrating PGCs is more frequently observed in the presence of FGFR inhibitor. (A) Fragmentation of a PGC (arrowed) is shown from a time-lapse movie of an E9.5 OCT4ΔPE:GFP embryo slice treated with 1 μM SU5402. The GFP-labeled PGC (arrow), started to fragment at frame 62, corresponding to 434 minutes from the beginning of movie. This time of onset of fragmentation is represented by the single dot with the red circle in D. (B) A fragmented PGC is stained by the apoptotic cell marker anti-cleaved caspase-3. (C) Pictures from frame 20 of a control and FGFR inhibitor-treated slice. Fragments of PGCs are observed in the dorsal body wall of the 1 μM FGFR inhibitor-treated slice (dashed circle). No fragmented PGCs are observed in the control slice. (D) Timing of onset of fragmentation of PGCs, taken from a total of seven movies for each treatment. The onset of fragmentation of each PGC is represented as a dot. Fragmentation of the arrowed PGC in A started at frame 62, and is represented by the single dot with the red circle. Inset shows the average number of fragmentations in a single movie (fragmented germ cells/movie). Data are means±s.e.m. from three separate experiments (n=7). Means with different letters were significantly different (P<0.05) from each other. Scale bars: 10 μm for A,B; 100 μm for C.

fragmentation was not due to death of the slice after several hours in culture. More germ cells underwent fragmentation in slices treated with SU5402 (Fig. 4C,D; see also Movies 1 and 2 in the supplementary material). Mean numbers of fragmentations in a single movie were 1.7±0.4 in control, and 4.7±0.5, 4.6±0.6 and 5.7±0.8 in 1, 2.5 and 10 μM FGFR inhibitor-treated slices, respectively. The most pronounced difference was observed in 10 μM SU5402 group, the fragmentation of germ cells in these embryo slices was approximately threefold higher (P<0.05) than in DMSO-treated controls. These data show that more germ cells undergo apoptosis when FGF signaling is reduced. By contrast, the mean number of fragmentations was 1.4±0.5 in 100 ng/ml FGF7-treated slices, although this result was not significant at the P=0.05 level. It is technically difficult to get more statistically significant data for this. Each movie is a single confocal slice (2 μM thick) and contains only a few germ cells. Therefore the numbers of germ cells seen fragmenting in controls is low (mean=1.7). It is difficult to get a statistically significant number lower than this using the methods available.

FGF2 affects process formation and motility in migratory PGCs

To test the effect of added FGF ligands and inhibitors on migratory properties of PGCs, we manually traced PGCs in time-lapse movies and obtained trajectories of all germ cells whose migratory routes remained in the confocal plane throughout the culture period (Fig. 5A). Examples of PGC trajectories are shown in Fig. 5B. In every treatment, PGCs divided into two bilateral streams, which migrated laterally towards the genital ridges, showing that the directionality of migration was not affected. This suggested that FGFs are not required to attract PGCs towards the genital ridges. However, cell trajectories were extended by treatment with 10 ng/ml FGF2, and shortened by treatment with 10 μM SU5402. To quantify this effect, we scored the velocity, direction and displacement (vectorial distance moved) of PGCs. Four to five movies from three separate experiments were analyzed for each treatment, and six to eight cells were tracked in a single movie (see Movies 1-4 in the supplementary material).

As shown in Fig. 5C, both the velocity and displacement of

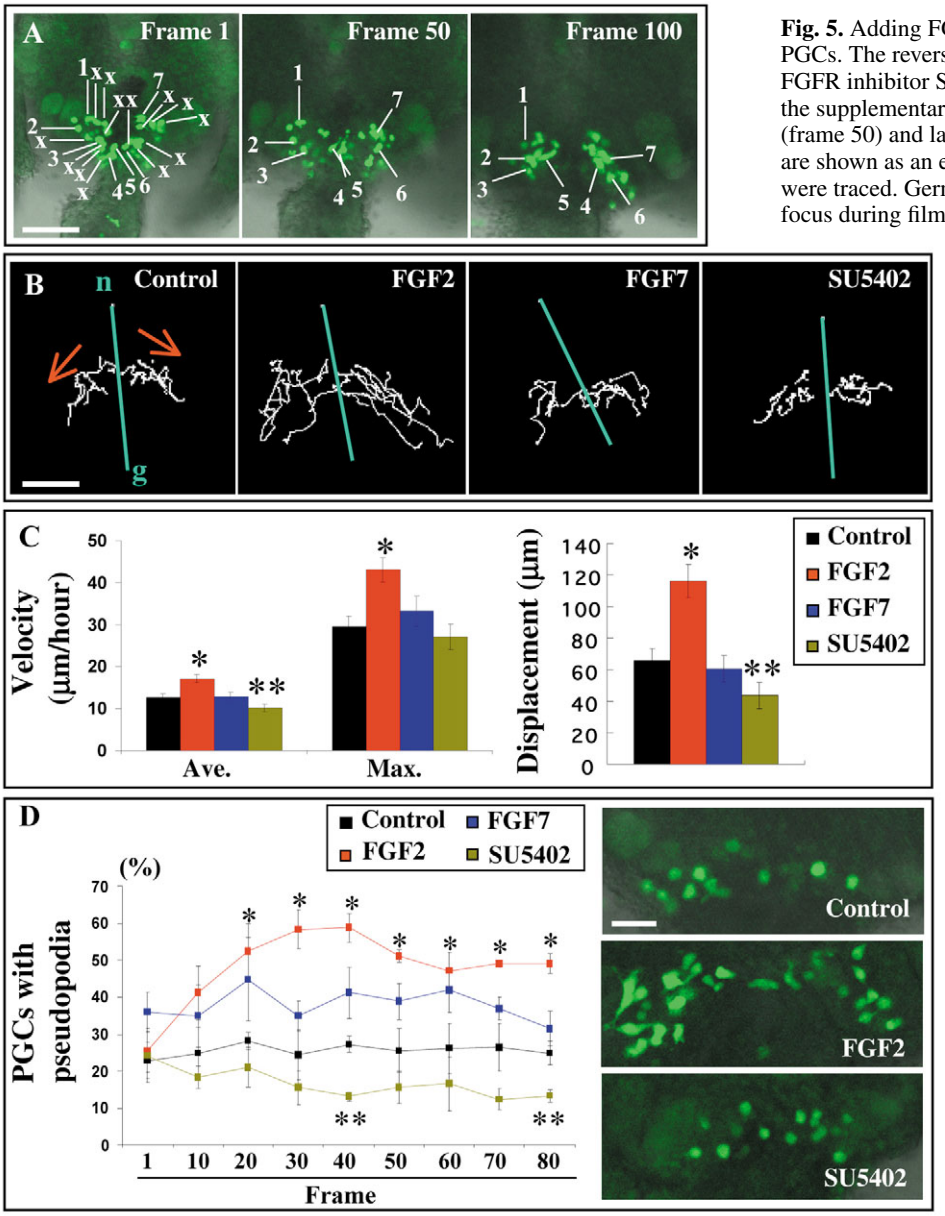

Fig. 5. Adding FGF2 to slices increased motility of migrating PGCs. The reverse effect was seen in slices cultured with the FGFR inhibitor SU5402. Time-lapse movies are available in the supplementary material. (A) The first (frame 1), middle (frame 50) and last (frame 100) frames from a single movie are shown as an example of cell tracing. Numbered germ cells were traced. Germ cells marked 'X' moved out of the plane of focus during filming, and were not traced. When PGCs divided, one of the siblings was traced. (B) Typical trajectories of migrating PGCs in controls, 10 ng/ml FGF2-treated slices, 100 ng/ml FGF7-treated slices and 10 μM SU5402-treated slices. Trajectories of PGCs were acquired using NIH image software. The green lines, connecting notochord (n) and the midline of hind gut (g), indicate the dorsoventral axis. Red arrows show the direction of PGC migration. In all treatments, PGCs showed directional movement towards the genital ridges. Trajectories were extended by FGF2 treatment, and shortened by SU5402 treatment. (C) Summary of PGC velocity data from six control, three FGF2- and FGF7-, and four SU5402-treated slices. Six to eight cells in each slice were analyzed. Mean, mean velocity for the whole culture period; Max., maximum velocity in any 35-minute period of culture. Error bars show the s.e.m. (D) PGCs exhibited exaggerated processes when exposed to FGF2. Every 10 frames, the percentage of PGCs showing processes was scored. In contrast to FGF-treatment, the formation of processes was inhibited in SU5402-treated slices. Pictures of PGCs taken from frame 40 of each treatment are shown in D. Asterisks in C and D indicate a degree of statistical significance (P<0.05) of increase (*) and decrease (**) compared with controls. Scale bars: 100 μm for A,B; 50 μm for D.

PGCs were significantly (P<0.05) increased by treatment with 10 ng/ml of FGF2. By contrast, they were significantly (P<0.05) decreased by 10 μM of SU5402. Neither of these parameters was affected by treatment with100 ng/ml of FGF7 (Fig. 5C) or lower doses of SU5402 (e.g. 1 or 2.5 μM) (data not shown), even in slices where there were increased numbers (see Fig. 3A) or increased fragmentation of PGCs (see Fig. 4D). Indeed, most PGCs showed processes and migrated normally in lower doses of SU5402, whereas dying PGCs stopped process formation and migration just before fragmentation. We cannot obtain long enough trajectories from germ cells, which died in the middle of movie, for calculating values of velocity and displacement. Therefore, the data from dying germ cells were not included in the migratory properties.

Interestingly, germ cells in FGF2-treated slices were more elongated than controls (Fig. 5D). To quantify this response, we scored every tenth frame (70-minute time intervals) from the first to the eightieth frame of the movies for the percentage of PGCs extending pseudopods. As shown in Fig. 5D, when embryo slices were exposed to FGF2, PGCs rapidly extended more pseudopodia than controls did in the first 30 frames of culture (see Movie 3 in the supplementary material). By contrast, elongation of cytoplasm was inhibited by SU5402, and most of the SU5402-treated PGCs showed a rounded-up morphology (Fig. 5D, see Movie 2 in the supplementary material). There was no statistically significant difference between control and FGF7-treated PGCs.

FGF2 treatment also caused the slices themselves to spread more rapidly than controls did on the substratum. This probably passively enhances the overall displacement of the germ cells during the culture period, in addition to their increased motility and process formation. However, the measurements of process formation (Fig. 5D) and velocity of individual germ cells (Fig. 5C) show that germ cell movement is enhanced by FGF2 treatment.

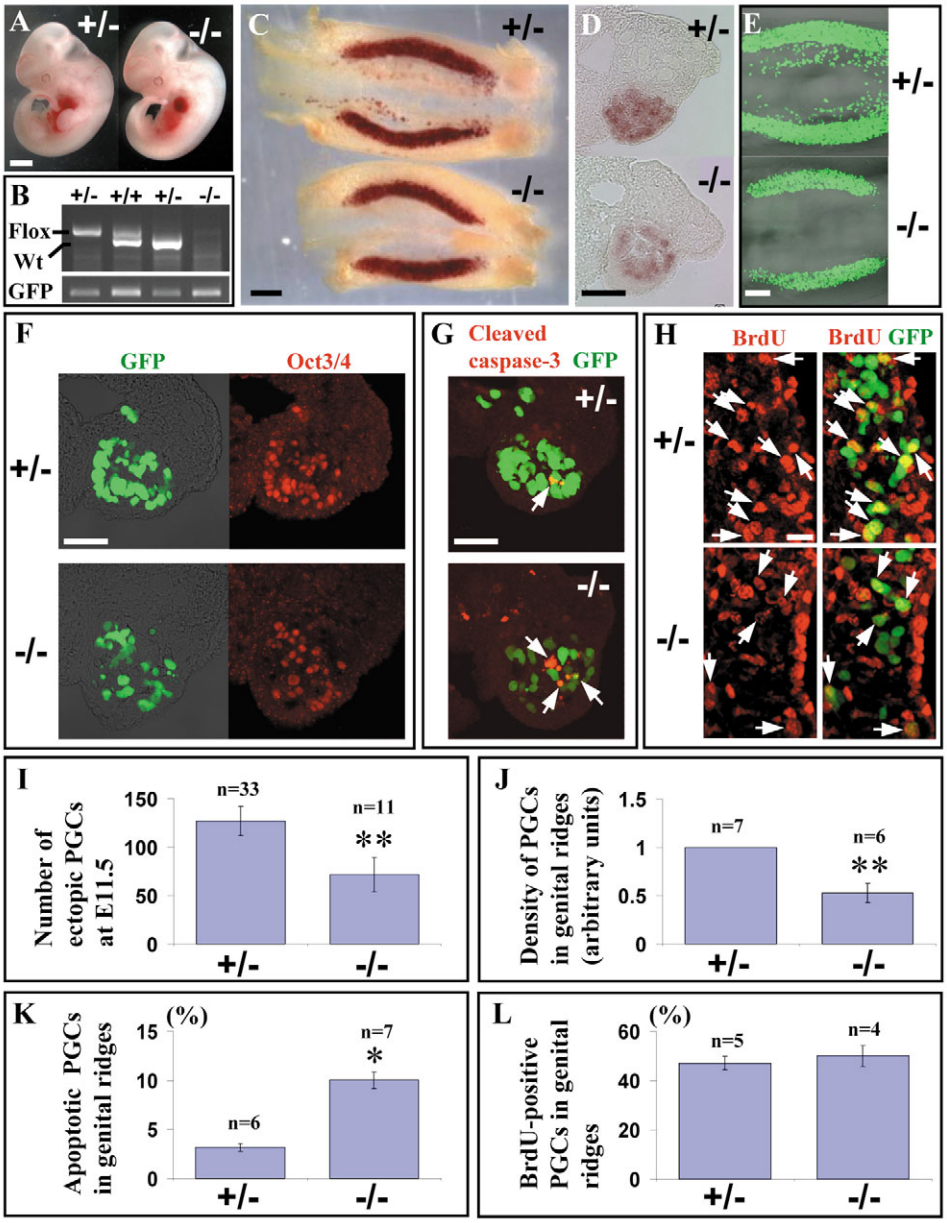

Fig. 6. Phenotypes of the FGFR2-IIIb$^{-/-}$ embryo. (A) Heterozygous and homozygous littermates at E11.5. Null embryos grow to the same size as heterozygotes at this stage, and are relatively normal, but they lack both fore and hind limbs. (B) Genotyping of embryos by genomic PCR. (C) Alkaline phosphatase (AP)-stained genital ridge and midline preparations are compared in E11.5 embryos. The numbers of ectopic PGCs were drastically reduced in null embryos. (D) Transverse section of AP-stained genital ridges showing a reduction of gonadal germ cells. (E) The targeted FGFR2-IIIb mutation was bred into the OCT4ΔPE:GFP mouse line. The same effect, reduction of ectopic germ cells, was seen in null embryos. (F) Transverse sections of genital ridges shown in E. Sections were stained with OCT3/4 antibody to analyze the density of gonadal germ cells. (G) Sagittal sections of genital ridges were stained for the apoptosis marker cleaved caspase-3 (red). Cleaved caspase-3-positive germ cells are compared in genital ridges at E11.5. (H) BrdU-positive germ cells (arrows) in E11.5 genital ridges of heterozygous and null embryos. (I) The number of ectopic germ cells in heterozygous and null embryos at E11.5. (J) Quantitation of germ cell density in genital rides at E11.5. Because the density of germ cells varied between littermates, the data obtained from null embryos were normalized to the heterozygous littermates. (K) Quantitation of germ cell death in genital ridges at E11.5. (L) Percentage of BrdU-positive germ cells in genital ridges at E11.5. There is no statistically significant difference between the percentage of BrdU-positive germ cells in null gonads and heterozygous gonads. Asterisks in I-K indicate the degree of statistical significance (P<0.05) of increase (*) and decrease (**) compared with heterzygotes. Scale bars: 1 mm for A; 200 μm for C,E; 50 μm for D,F,G; 20 μm for H.

Targeted mutation of FGFR2-IIIb confirms a role for FGF signaling in maintaining germ cell numbers

To confirm in vivo the role suggested by slice culture experiments in vitro, we examined the numbers and positions of germ cells in litters of E11.5 embryos containing targeted mutations in FGFR2-IIIb. Homozygous mutant embryos are easy to score, because they lack fore and hind limbs (Fig. 6A), as reported previously (De Moerlooze et al., 2000). The dorsal body wall, including the genital ridges, of each embryo was dissected whole, fixed, and stained for alkaline phosphatase (AP), whilst the corresponding anterior end was genotyped (Fig. 6B). The most obvious effect of loss of FGFR2-IIIb at E11.5, visible in AP-stained whole mounts, was the dramatic reduction of ectopic germ cells (Fig. 6C). Normally, significant numbers of migrating germ cells do not reach the genital ridges, instead they remain scattered, as ectopic germ cells, close to the genital ridges, lateral to the midlines (see upper panel in Fig. 6C). In the analysis of six independent litters, which included 33 heterozygotes and 11 mutants, we observed a 46±10% reduction of ectopic germ cells in FGFR2-IIIb$^{-/-}$ embryos at E11.5 (Fig. 6I). Transverse sections of AP-stained genital ridges suggested that the density of gonadal germ cells was also reduced in FGFR2-IIIb$^{-/-}$ embryos (Fig. 6D).

The targeted FGFR2-IIIb mutation was bred into the OCT4ΔPE:GFP mouse line to enable us to analyze migration and germ cell numbers more accurately. Here, the same effect on ectopic germ cells was seen (Fig. 6E). The density of gonadal germ cells was assayed using anti-OCT3/4 antibody-stained transverse frozen sections (Fig. 6F). Each section was optically sectioned (z=6 μm). In the bright-field images, the

borders between the genital ridges and the surrounding somatic cells, such as epithelium and mesenchyme, could be clearly seen. The genital ridge of each confocal image in the *z*-stacks was measured using the Zeiss software, and then multiplied by the thickness of the *z*-stacks to give the volumes of the genital ridge contained in the *z*-stacks. The number of germ cells was then divided by the volume of the genital ridge to obtain the density of gonadal germ cells. For example, the density (±s.e.m.) of gonadal germ cells was estimated as 560,494±31,377 cells/mm^3 (n=7) and 189,773±18,200 cells/mm^3 (n=6) in heterozygous and mutant embryos, respectively. Because the density of germ cells varied between litters, data from three different litters were normalized to the corresponding heterozygous embryos to allow incorporation into a single figure. As shown in Fig. 6J, gonadal germ cells from FGFR2-IIIb$^{-/-}$ embryos had a mean density (cells/mm^3) that was 45% of that of heterozygous gonads. As seen in Fig. 6C-G, the sizes of the genital ridges in FGFR2-IIIb null embryos were comparable to those of wild-type littermates. This suggests that the FGFR2-IIIb null mutation did not affect the formation of the genital ridges. Taken together, overall germ cell numbers, not just those of ectopic germ cells, were reduced at E11.5 in the absence of FGF signaling through FGFR2-IIIb. Reductions in the numbers of gonadal germ cells in mutant gonads were also observed by immunostaining with another germ cell marker, SSEA-1 (FUT4 – Mouse Genome Informatics; data not shown).

To distinguish between the affects on proliferation and apoptosis of germ cells in the absence of FGFR2-IIIb, cell death and proliferation were examined in heterozygotes and mutants at E11.5 using cleaved caspase-3 staining (Fig. 6G) and BrdU incorporation assays (Fig. 6H). The percentage of cleaved caspase-3-positive or BrdU-positive germ cells was counted in four sections per embryo from each of three independent litters. Significant differences (P<0.05) in the numbers of cleaved caspase-3-positive cells were seen in heterozygous and null genital ridges [1.9±0.6% in heterozygotes (n=6) versus 7.3±0.8% in nulls (n=7); Fig. 6G,K]. However, similar proportions of BrdU-positive germ cells were seen in both heterozygous and null genital ridges (Fig. 6H,L). Our data show that E11.5 gonadal germ cells do not require FGFR2-IIIb to maintain normal rates of proliferation, but that the number of germ cells undergoing apoptosis in the genital ridges increases in the absence of this signaling. These in vivo results are consistent with the effects seen using gain- and loss-of-function experiments in slice cultures.

Discussion

FGF signaling is known to be an essential factor for the migration of embryonic cells in multicellular organisms, such as tracheal cells and glial cells in *Drosophila* (Klämbt et al., 1992), and sex myoblasts in *C. elegans* (DeVore et al., 1995). However, the roles in germ cell migration of members of the FGF family of growth factors are not yet understood. Here, we functionally analyze the roles of FGF signaling during migration in the embryo, by showing: (1) that migrating mouse PGCs express two FGFRs (*Fgfr1-IIIc* and *Fgfr2-IIIb*); (2) that FGF signaling activates the MEK-ERK pathway, a major downstream MAP kinase cascade of FGF signaling, in an FGF-dependent manner; and (3) that the MAPK pathway in migrating PGCs is upregulated by adding exogenous FGFs, or downregulated by soluble FGF inhibitors. Furthermore, we show that the principal in vivo roles for FGF signaling via FGFR1-IIIc and FGFR2-IIIb are to control germ cell migration and cell shape change, and germ cell numbers, respectively, rather than mitogenesis. Finally, we found that PGC numbers are dramatically decreased in mouse embryos deficient for FGFR2-IIIb, and show increased incidence of apoptosis in the early genital ridges.

In this paper, we identified the FGFRs expressed by PGCs during migration and focussed on the roles of these receptors in PGC development. It is difficult to identify which FGF ligands are responsible for the activation of these receptors in vivo, because the FGF protein family consists of at least 22 members (in humans), and FGFs within each subfamily have similar receptor-binding properties and over-lapping patterns of expression (Ornitz and Itoh, 2001). Functional redundancy is therefore likely to occur in mice containing targeted mutations in individual FGF genes. For example, FGF2 is known to be an essential factor promoting PGC proliferation in vitro (Matsui et al., 1992; Resnick et al., 1998). However, mice deficient for FGF2 or for both FGF1 and FGF2 are fertile (Zhou et al., 1998; Miller et al., 2000). Whole-mount in situ hybridization studies for FGFs in mouse embryos showed that FGF3, FGF4, FGF8, FGF10 and FGF17 are expressed in neighboring somatic tissue along the migratory route of PGCs (Wright and Mansour, 2003; Kawase et al., 2004). It is known that FGF4, FGF8 and FGF17 (epithelial FGFs), and FGF3 and FGF10 (mesenchymal FGFs), can activate FGFR1-IIIc and FGFR2-IIIb, respectively (Powers et al., 2000). Therefore, these FGFs could act as the physiological ligands for migrating PGCs in vivo. Although PGCs start expressing FGF4 and FGF8 after they colonized the genital ridges (Kawase et al., 2004), no FGF ligands have been identified as being expressed by migrating PGCs so far (Y.T. and C.W., unpublished).

It has been shown that FGF2 and FGF4 stimulate PGC proliferation in culture (Matsui et al., 1992; Resnick et al., 1998; Kawase et al., 2004). However, we show here that addition of FGF2 and FGF7 did not increase BrdU incorporation in PGCs, and PGCs continued to divide and take up BrdU in the absence of FGF signaling in cultured slices. In addition, BrdU incorporation by PGCs was not affected in FGFR2-IIIb-deficient mice, although PGC number was reduced in this mutant. These data suggest that FGF signaling via either FGFR1-IIIc or FGFR2-IIIb does not stimulate mitogenic activity in PGCs in vivo. It is not clear why the addition of FGF2 should cause different effects in germ cells in embryo slices and in germ cells dissociated and cultured on feeder layers. It may be that the feeder cells provide additional signals, or that the cell contact phenomena are different, and modulate different responses. Addition of FGF2 and FGF7, respectively, to embryo slice cultures had different effects. FGF2 increased motility and process formation, whereas FGF7 increased germ cell numbers but had no effect on motility. Addition of the FGF receptor-blocking agent SU5402 caused a dose-dependent decrease in germ cell numbers, and a decrease in motility at high doses but not low doses. It is not clear why SU5402 did not affect motility at lower doses. It may be that different threshold reductions in FGF receptor activity are required for different FGF-mediated functions, or that

different levels of the ligands for each of the receptors are present. We conclude from this data that signaling through the FGFR1-IIIc receptor, either in germ cells themselves or in adjacent somatic cells, controls germ cell motility, whilst signaling through the FGFR2-IIIb receptor controls germ cell survival. Genetic loss-of-function data in FGFR2-IIIb embryos supports this proposed role in germ cell survival.

Global knockouts of FGFR1 (both of the b and c forms) and FGFR1-IIIc mice die late in gastrulation, too early for the effects on PGC migration to be assessed, and thus they do not test the proposed role for FGFR1-IIIc in germ cell migration. However, they do show defects in mesoderm cell migration and specification (Yamaguchi et al., 1994; Partanen et al., 1998). Furthermore, it is shown that FGFR1$^{-/-}$ cells overexpress E-cadherin, and that this expression is accompanied by the downregulation of mouse *Snail* (Ciruna et al., 1997). In the present paper, we studied that the role of FGF signaling via FGFR1-IIIc by adding its potential ligand FGF2, and the loss-of-function by adding the global inhibitor of FGF/FGFR signaling SU5402. Germ cells extended exaggerated processes when treated with FGF2, which correlated with an upregulation of their migratory activity, as analyzed by time-lapse movies. The reverse effects were seen following FGFR inhibitor treatment. These data strongly suggest that FGFR1-IIIc signaling is required for PGC migration and/or the establishment of cell-cell communications using pseudopodia.

The data here do not address whether FGFR1-IIIc- or FGFR2-IIIb-mediated events occur by direct ligand-receptor interaction on germ cells, on adjacent somatic cells, or on both. PGC-specific depletion of both receptors during migration by a conditional *Cre/loxP* gene targeting strategy will be required to examine the cell specificities of these pathways.

Defects in PGC migration underlie many human congenital disorders. For example, extra-gonadal germ cell tumors are thought to arise from PGCs that do not migrate correctly into the genital ridges and that fail to die (Upadhyay and Zamboni, 1982; Gobel et al., 2000). Therefore, it will be important to study the downstream targets of FGFR1-IIIc and FGFR2-IIIb activation to understand the mechanisms that control process formation and apoptosis of germ cells. In particular, the mechanism of cell death of ectopic germ cells caused by the mis- or incomplete migration of PGCs is not well understood to date. Future work will focus on trying to understand how germ cell survival is controlled by FGF signaling.

We thank C. Dickson for supplying the FGFR2-IIIb floxed mice. We also thank members of M. Nakafuku's laboratory for their outstanding advice concerning the fluorescent immunostaining. This work was supported by the NIH (R01-HD33440).

Supplementary material

Supplementary material for this article is available at
http://dev.biologists.org/cgi/content/full/132/24/5399/DC1

References

Anderson, R., Fassler, R., Georges-Labouesse, E., Hynes, R. O., Bader, B. L., Kreidberg, J. A., Schaible, K., Heasman, J. and Wylie, C. (1999). Mouse primordial germ cells lacking beta1 integrins enter the germline but fail to migrate normally to the gonads. *Development* **126**, 1655-1664.

Araki, K., Araki, M., Miyazaki, J. and Vassalli, P. (1995). Site-specific recombination of a transgene in fertilized eggs by transient expression of Cre recombinase. *Proc. Natl. Acad. Sci. USA* **92**, 160-164.

Bennett, D. (1956). Developmental analysis of a mutation with the pleiotropic effects in the mouse. *J. Morphol.* **98**, 57-70.

Bernard-Pierrot, I., Ricol, D., Cassidy, A., Graham, A., Elvin, P., Caillault, A., Lair, S., Broet, P., Thiery, J. P. and Radvanyi, F. (2004). Inhibition of human bladder tumour cell growth by fibroblast growth factor receptor 2b is independent of its kinase activity. Involvement of the carboxy-terminal region of the receptor. *Oncogene* **23**, 9201-9211.

Bridges, J. P., Wert, S. E., Nogee, L. M. and Weaver, T. E. (2003). Expression of a human surfactant protein C mutation associated with interstitial lung disease disrupts lung development in transgenic mice. *J. Biol. Chem.* **278**, 52739-52746.

Ciruna, B. G., Schwartz, L., Harpal, K., Yamaguchi, T. P. and Rossant, J. (1997). Chimeric analysis of fibroblast growth factor receptor-1 (Fgfr1) function: a role for FGFR1 in morphogenetic movement through the primitive streak. *Development* **124**, 2829-2841.

Corson, L. B., Yamanaka, Y., Lai, K. M. and Rossant, J. (2003). Spatial and temporal patterns of ERK signaling during mouse embryogenesis. *Development* **130**, 4527-4537.

De Felici, M. (2000). Regulation of primordial germ cell development in the mouse. *Int. J. Dev. Biol.* **44**, 575-580.

De Moerlooze, L., Spencer-Dene, B., Revest, J., Hajihosseini, M., Rosewell, I. and Dickson, C. (2000). An important role for the IIIb isoform of fibroblast growth factor receptor 2 (FGFR2) in mesenchymal-epithelial signalling during mouse organogenesis. *Development* **127**, 483-492.

DeVore, D. L., Horvitz, H. R. and Stern, M. J. (1995). An FGF receptor signaling pathway is required for the normal cell migrations of the sex myoblasts in *C. elegans* hermaphrodites. *Cell* **83**, 611-620.

Gobel, U., Schneider, D. T., Calaminus, G., Haas, R. J., Schmidt, P. and Harms, D. (2000). Germ-cell tumors in childhood and adolescence. GPOH MAKEI and the MAHO study groups. *Annu. Oncol.* **11**, 263-271.

Godin, I., Wylie, C. and Heasman, J. (1990). Genital ridges exert long-range effects on mouse primordial germ cell numbers and direction of migration in culture. *Development* **108**, 357-363.

Godin, I., Deed, R., Cooke, J., Zsebo, K., Dexter, M. and Wylie, C. C. (1991). Effects of the steel gene product on mouse primordial germ cells in culture. *Nature* **352**, 807-809.

Kawase, E., Hashimoto, K. and Pedersen, R. A. (2004). Autocrine and paracrine mechanisms regulating primordial germ cell proliferation. *Mol. Reprod. Dev.* **68**, 5-16.

Klämbt, C., Glazer, L. and Shilo, B. Z. (1992). *breathless*, a Drosophila FGF receptor homolog, is essential for migration of tracheal and specific midline glial cells. *Genes Dev.* **6,** 1668-1678.

Matsui, Y., Zsebo, K. and Hogan, B. L. (1992). Derivation of pluripotential embryonic stem cells from murine primordial germ cells in culture. *Cell* **70**, 841-847.

Miller, D. L., Ortega, S., Bashayan, O., Basch, R. and Basilico, C. (2000). Compensation by fibroblast growth factor 1 (FGF1) does not account for the mild phenotypic defects observed in FGF2 null mice. *Mol. Cell. Biol.* **20**, 2260-2268.

Mintz, B. and Russel, E. S. (1957). Gene-induced embryological modifications of primordial germ cells in the mouse. *J. Exp. Zool.* **134**, 207-237.

Mohammadi, M., McMahon, G., Sun, L., Tang, C., Hirth, P., Yeh, B. K., Hubbard, S. R. and Schlessinger, J. (1997). Structures of the tyrosine kinase domain of fibroblast growth factor receptor in complex with inhibitors. *Science* **276**, 955-960.

Molyneaux, K. and Wylie, C. (2004). Primordial germ cell migration. *Int. J. Dev. Biol.* **48**, 537-544.

Molyneaux, K. A., Stallock, J., Schaible, K. and Wylie, C. (2001). Time-lapse analysis of living mouse germ cell migration. *Dev. Biol.* **240**, 488-498.

Molyneaux, K. A., Zinszner, H., Kunwar, P. S., Schaible, K., Stebler, J., Sunshine, M. J., O'Brien, W., Raz, E., Littman, D., Wylie, C. et al. (2003). The chemokine SDF1/CXCL12 and its receptor CXCR4 regulate mouse germ cell migration and survival. *Development* **130**, 4279-4286.

Molyneaux, K. A., Wang, Y., Schaible, K. and Wylie, C. (2004). Transcriptional profiling identifies genes differentially expressed during and after migration in murine primordial germ cells. *Gene Expr. Patterns* **4**, 167-181.

Ornitz, D. M. and Itoh, N. (2001). Fibroblast growth factors. *Genome Biol.* **2**, 3005.1-3005.12.

Partanen, J., Schwartz, L. and Rossant, J. (1998). Opposite phenotypes of hypomorphic and Y766 phosphorylation site mutations reveal a function for

Fgfr1 in anteroposterior patterning of mouse embryos. *Genes Dev.* **12**, 2332-2344.

Pesce, M., Farrace, M. G., Piacentini, M., Dolci, S. and De Felici, M. (1993). Stem cell factor and leukemia inhibitory factor promote primordial germ cell survival by suppressing programmed cell death (apoptosis). *Development* **118**, 1089-1094.

Powers, C. J., McLeskey, S. W. and Wellstein, A. (2000). Fibroblast growth factors, their receptors and signaling. *Endocr. Relat. Cancer* **7**, 165-197.

Resnick, J. L., Ortiz, M., Keller, J. R. and Donovan, P. J. (1998). Role of fibroblast growth factors and their receptors in mouse primordial germ cell growth. *Biol. Reprod.* **59**, 1224-1229.

Stallock, J., Molyneaux, K., Schaible, K., Knudson, C. M. and Wylie, C. (2003). The pro-apoptotic gene Bax is required for the death of ectopic primordial germ cells during their migration in the mouse embryo. *Development* **130**, 6589-6597.

Sher, I., Yeh, B. K., Mohammadi, M., Adir, N. and Ron, D. (2003). Structure-based mutational analyses in FGF7 identify new residues involved in specific interaction with FGFR2IIIb. *FEBS Lett.* **552**, 150-154.

Upadhyay, S. and Zamboni, L. (1982). Ectopic germ cells: natural model for the study of germ cell sexual differentiation. *Proc. Natl. Acad. Sci. USA* **79**, 6584-6588.

Weksler, N. B., Lunstrum, G. P., Reid, E. S. and Horton, W. A. (1999). Differential effects of fibroblast growth factor (FGF) 9 and FGF2 on proliferation, differentiation and terminal differentiation of chondrocytic cells in vitro. *Biochem. J.* **342**, 677-682.

Wright, T. J. and Mansour, S. L. (2003). Fgf3 and Fgf10 are required for mouse otic placode induction. *Development* **130**, 3379-3390.

Yamaguchi, T. P., Harpal, K., Henkemeyer, M. and Rossant, J. (1994). *fgfr-1* is required for embryonic growth and mesodermal patterning during mouse gastrulation. *Genes. Dev.* **8**, 3032-3044.

Zhou, M., Sutliff, R. L., Paul, R. J., Lorenz, J. N., Hoying, J. B., Haudenschild, C. C., Yin, M., Coffin, J. D., Kong, L., Kranias, E. G. et al. (1998). Fibroblast growth factor 2 control of vascular tone. *Nat. Med.* **4**, 201-207.